Environmental Science & Technology

Article

Cite This: Environ. Sci. Technol. 2018, 52, 581−588

pubs.acs.org/est

Selenium(IV) Sorption Onto γ-Al_2O_3: A Consistent Description of the Surface Speciation by Spectroscopy and Thermodynamic Modeling

Natalia Mayordomo,[†] Harald Foerstendorf,*[,‡] Johannes Lützenkirchen,[§] Karsten Heim,[‡] Stephan Weiss,[‡] Ursula Alonso,[†] Tiziana Missana,[†] Katja Schmeide,[‡] and Norbert Jordan*[,‡]

[†]CIEMAT, Department of Environment, Avenida Complutense 40, CP 28040, Madrid, Spain

[‡]Helmholtz-Zentrum Dresden - Rossendorf (HZDR), Institute of Resource Ecology, Bautzner Landstraße 400, 01328 Dresden, Germany

[§]Institute for Nuclear Waste Disposal, Karlsruhe Institute of Technology, Hermann-von-Helmholtz Platz 1, 76344 Eggenstein-Leopoldshafen, Germany

Supporting Information

ABSTRACT: The sorption processes of Se(IV) onto γ-Al_2O_3 were studied by in situ Infrared spectroscopy, batch sorption studies, zeta potential measurements and surface complexation modeling (SCM) in the pH range from 5 to 10. In situ attenuated total reflection fourier-transform infrared (ATR FT-IR) spectroscopy revealed the predominant formation of a single inner-sphere surface species at the alumina surface, supporting previously reported EXAFS results, irrespective of the presence or absence of atmospherically derived carbonate. The adsorption of Se(IV) decreased with increasing pH, and no impact of the ionic strength was observed in the range from 0.01 to 0.1 mol L^{-1} NaCl. Inner-sphere surface complexation was also suggested from the shift of the isoelectric point of γ-Al_2O_3 observed during zeta potential measurements when Se(IV) concentration was 10^{-4} mol L^{-1}. Based on these qualitative findings, the acid−base surface properties of γ-Al_2O_3 and the Se(IV) adsorption edges were successfully described using a 1-p*K* CD-MUSIC model, considering one bidentate surface complex based on previous EXAFS results. The results of competitive sorption experiments suggested that the surface affinity of Se(IV) toward γ-Al_2O_3 is higher than that of dissolved inorganic carbon (DIC). Nevertheless, from the in situ experiments, we suggest that the presence of DIC might transiently impact the migration of Se(IV) by reducing the number of available sorption sites on mineral surfaces. Consequently, this should be taken into account in predicting the environmental fate of Se(IV).

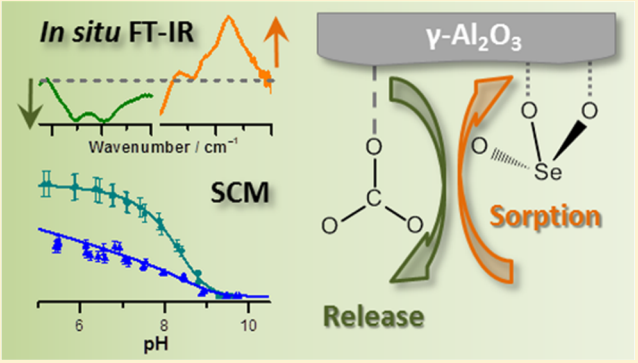

INTRODUCTION

Selenium (Se) is present in the environment due to natural or anthropogenic sources (e.g., the use of fertilizers).[1] Selenium removal is a matter of concern because it represents health hazards for living organisms.[2] Under near-neutral pH and slightly reducing conditions, the hydrogenselenite ($HSeO_3^-$) and selenite (SeO_3^{2-}) anions are the most stable chemical species in aqueous solutions.[3] Consequently, understanding the fate of selenium in the environment and the processes governing its migration are of high importance.

Adsorption onto colloidal particles (e.g., iron oxyhydroxides or clays), which are ubiquitous in the environment, is a process potentially facilitating the dissemination of selenium. Gamma alumina (γ-Al_2O_3) has been widely used in different industrial and research applications (e.g., as catalytic support) due to its surface characteristics,[4] although it is metastable with respect to other aluminum (hydro)oxide phases.[5] Considering rising demand, it is likely that nano γ-alumina can be released into the bio/geosphere. γ-Al_2O_3 is also a good candidate to sorb anions within a wide range of pH conditions, because of its amphoteric behavior and high point of zero charge ($pH_{PZC} \approx 8-9$).[6−8] Furthermore, γ-Al_2O_3 can be used as a model oxide for clay minerals, since alumina expose surface functional groups comparable to those present at the edge of clay particles.[9]

Identifying the surface interactions at a molecular scale is of interest since the type of surface complexation affects the reversibility of the sorption processes and, thus, the retention capability. X-ray absorption spectroscopy (XAS) has been previously applied to get insights on the Se(IV) surface speciation on γ-alumina.[10] The formation of bidentate bridging complexes with AlO_6 surface groups between pH 4 and 8 was observed. The possibility of additional outer-sphere Se(IV) complexes at the γ-Al_2O_3 surface was not completely ruled out, however.[10]

Received: September 4, 2017
Revised: December 11, 2017
Accepted: December 11, 2017
Published: December 12, 2017

DOI: 10.1021/acs.est.7b04546
Environ. Sci. Technol. 2018, 52, 581−588

Accurate knowledge about the occurring surface processes is mandatory for a robust thermodynamic description based on surface complexation modeling, to constrain the number of surface species and their stoichiometry.

Under groundwater conditions, Se(IV) coexists with other anions (SO_4^{2-}, Cl^-, and NO_3^-), which in principle will be competing for sorption sites on (Fe, Al) oxides surfaces.[11−14] On such surfaces, the sorption of Se(IV) was found to be significantly impacted and decreased in the presence of such competitors, depending on the competitor to selenium concentration ratio, and on the prevailing pH. However, to the best of our knowledge, less attention has been paid to the competing effect of dissolved inorganic carbon (DIC) on Se(IV) surface coordination and reversibility.

In this work, in situ attenuated total reflection fourier-transform infrared (ATR FT-IR) spectroscopy[15−17] was applied to identify Se(IV) surface complexes on the γ-Al_2O_3 surface, and to thereby understand molecular interactions as well as sorption and desorption processes including the impact of carbonate at different pH values and ionic strengths. At the macroscopic scale, batch studies and zeta potential measurements were performed in order to investigate the impact of pH and ionic strength on the sorption of Se(IV) onto γ-Al_2O_3. Potentiometric titrations and zeta potential measurements were carried out and the acid−base surface properties of γ-Al_2O_3 were modeled using a 1-p*K* CD-MUSIC approach. The derived properties (binding electrolyte constants and capacitances) were then used to describe Se(IV) adsorption edges and the isoelectric points, constraining surface speciation based on the IR investigations.

MATERIALS AND METHODS

γ-Al_2O_3 Nanoparticles Characterization. γ-Al_2O_3 nanoparticles (>99% purity, Aldrich) from two batches with nominal diameter <50 nm were used. The first batch was used for the potentiometric titrations, zeta potential and Se(IV) adsorption edges. The specific surface area of this batch (Multipoint Beckman Coulter surface analyzer SA 3100) was determined to be 127 $m^2\ g^{-1}$ by applying the Brunauer−Emmett−Teller (BET) equation with nitrogen adsorption isotherms at 77 K. Characterization details of the second batch exclusively used for the spectroscopic investigations were presented elsewhere.[14] The N_2−BET specific surface area of this sample was 136 $m^2\ g^{-1}$ and its isoelectric point pH_{IEP} equal to 8.5. XRD measurements confirmed the purity of γ-Al_2O_3 and the absence of other Al-phases such as bayerite, gibbsite, etc. in both batches (Figure S1, Supporting Information (SI)).

Several studies highlighted the transformation of γ-Al_2O_3 at room temperature and in aqueous suspensions after a few days into Al (oxy)hydroxides.[18−22] The γ-Al_2O_3 sample (batch 1) was equilibrated for three and seven days in 0.1 mol L^{-1} NaCl. After freeze-drying, samples were analyzed by XRD and IR spectroscopy. No significant differences compared to the raw material were observed (SI Figures S2 and S3). During the in situ ATR FT-IR sorption studies, the same suspension was used for all experiments and no hints for surface alterations with time (over two months) were noticed. Consequently, bulk and surface transformations of γ-Al_2O_3 were not observed under our experimental conditions. This apparent contradiction with former studies[18−22] might arise from differences in the surface to bulk ratios.

For the modeling purposes, surface acid−base properties of γ-Al_2O_3 were comprehensively characterized by potentiometric titrations and zeta potential studies. Potentiometric titrations (pH range 5−9.5) were performed at different ionic strengths of NaCl (0.1, 0.05, and 0.01 mol L^{-1}) with a Metrohm 736 GP Titrino titrator. For each titration, a 20 g L^{-1} suspension of γ-Al_2O_3 (50 mL volume) was inserted in a borosilicate vessel and equilibrated overnight at pH ∼ 5. A continuous argon flux (Argon N50 from Air Liquide) was streamed over the suspension to avoid dissolution of atmospheric CO_2. To ensure a homogeneous suspension, a Teflon propeller was used. After overnight pre-equilibration, base titration was performed by addition of aliquots (20 μL) of 0.1 mol L^{-1} NaOH. The pH electrode (Schott BlueLine 11pH) was calibrated using a three point calibration with buffer solutions (pH 4.01, 6.87, and 9.18). Zeta potential measurements were also performed using a Laser-Doppler-Electrophoresis instrument (nano-ZS, Malvern Instruments Ltd.), under CO_2 exclusion, at a mass to volume ratio m/v = 0.25 g L^{-1} and at two ionic strengths (0.005 and 0.01 mol L^{-1} NaCl).

Solutions. Detailed descriptions of the preparation of the solutions are given in the SI.

ATR FT-IR Experiments. The in situ IR spectroscopic experiments allowed a monitoring of the sorption and desorption processes on solid phase surfaces. For this, a mineral film was prepared as a stationary phase directly onto the surface of the ATR crystal by repeatedly pipetting aliquots of 1 μL from a suspension (2.5 g L^{-1} γ-Al_2O_3 in deionized Milli-Q water) and subsequently evaporating the solvent by gentle drying with $N_2(g)$. The amount of alumina on the crystal surface was verified by the transmission of the IR light which was not allowed to fall below a value of ∼15% in the mid-IR frequency region. Subsequently, a flow cell was mounted which was connected to a peristaltic pump providing a continuous flow rate of 100 mL min^{-1} from the reservoirs containing the solutions of the background electrolyte or of the sorbate, that is Se(IV) or DIC. A valve allows the selection of the respective solution to be flushed through the setup.

Sorption and desorption experiments were monitored by continuously measuring IR single beam spectra during three sequential steps of the experiment, that is (i) equilibration, (ii) sorption and (iii) flushing/desorption as described earlier.[15,16] During the equilibration step, the stationary phase was flushed with a blank solution only containing the background electrolyte for at least 60 min until spectral changes minimized. Subsequently, sorption was induced by switching to the respective solution containing the sorbate until no further spectral changes occurred. Finally, desorption was induced by switching back to the blank solution. This setup allowed to induce adsorption and desorption processes of Se(IV) in the presence or absence of DIC. Moreover, both anions could be optionally added consecutively or simultaneously providing insight into competitive processes of both anions at the solid−liquid interface. With respect to the absorption properties of the aqueous phase, the relatively low concentrations and the characteristic frequency ranges of the vibrational modes of the Se(IV) and HCO_3^- anions, that is, 1000−600 cm^{-1} and 1600−1300 cm^{-1}, the experiments had to be performed in D_2O and H_2O, respectively. In D_2O, the pD was calculated by the following equation:[23]

$$pD = pH_{meter\ reading} + 0.4$$

All IR experiments were performed with a Bruker Vertex 80/v spectrometer equipped with a horizontal ATR diamond crystal (SamplIIR II, Smiths inc., 9 reflections, 45° angle of incidence) and a Mercury Cadmium Telluride detector with a low frequency cutoff at 580 cm^{-1}. Spectral resolution was 4 cm^{-1} and the spectra were averaged over 256 scans. All manipulations of the spectra were accomplished with the OPUS software.[15,16]

DOI: 10.1021/acs.est.7b04546
Environ. Sci. Technol. 2018, 52, 581−588

Further details of the acquisition of reference spectra are given in the SI.

Batch Sorption and Zeta Potential Studies. γ-Al_2O_3 (10 mg) was suspended in 40 mL of NaCl solution in 50 mL polypropylene tubes resulting in m/v = 0.25 g L^{-1}. Two background electrolyte concentrations were used, that is, 0.1 and 0.01 mol L^{-1}. The initial Se(IV) concentrations were 10^{-5} and 10^{-4} mol L^{-1}. The pH of the alumina suspensions was adjusted by addition of HCl or NaOH and was recorded after being stable for more than 10 min. Experiments were performed in a glovebox in N_2 atmosphere (O_2 < 5 ppm). After 3 days of equilibration, samples were centrifuged for 2 h at 6800*g* (Avanti J-20 XP Beckman Coulter) and the remaining selenium concentration in the supernatants was determined by inductively coupled plasma mass spectrometry (ICP-MS, PerkinElmer ELAN 9000). All the experiments were carried out in duplicate. Zeta potential measurements were carried out on the same suspensions (prior to the centrifugation), the measuring cell being filled in a glovebox under a N_2 atmosphere. A more detailed description of the instrumental analytic techniques applied can be found elsewhere.[24]

Surface Complexation Modeling. The most frequently used model to describe the surface of γ-Al_2O_3 consists of five different kinds of OH groups, namely $Al^{IV}OH^{-0.25}$, $Al^{VI}OH^{-0.25}$, $[Al^{IV}-OH-Al^{VI}]^{+0.25}$, $[Al^{VI}-OH-Al^{VI}]^{0}$ and $[Al^{VI}-OH-(Al^{VI})_2]^{+0.5}$, derived from IR and NMR studies.[4]

The surface properties of γ-Al_2O_3 using one equivalent site $\equiv SO^{-0.5}$ representing the acidic groups $Al^{IV}OH^{-0.25}$, $Al^{IV}Al^{VI}O^{-0.75}$ and $Al^{VI}{}_3O^{-0.5}$, as well as one site $\equiv AlOH^{-0.5}$ with singly coordinated hydroxyl groups were described previously.[25] 25% of both types of sites were assumed to be located in the subsurface. Satisfactory results were obtained by assuming charge penetration of both Na and Cl electrolyte ions for the subsurface sites. A total site density of 6.6 sites nm^{-2} (2.5 for each normal site and 0.8 for each subsurface site) was used by Hiemstra et al.[25]

As shown later, a pragmatic approach considering one site $\equiv AlOH^{-0.5}$ (thought to represent singly coordinated hydroxyl groups with fractional charges) is sufficient to provide an adequate description of the surface properties of γ-Al_2O_3. A surface site density of 7 sites nm^{-2} was chosen in this study, close to the total surface site density used by Hiemstra et al.[25]

Surface complexation modeling was performed using the CD-MUSIC model with a one-p*K* approach.[26] The titration and zeta potential data for the sorbent were modeled using one site as discussed above with a p*K* equal to 9.0. Since a better description of the data in comparison to a two plane model (Basic Stern) could be obtained, a three plane model with electrolyte binding in the plane 2 (head-end of the diffuse layer) was used. The adjustable parameters were the two electrolyte association constants (Na^+ and Cl^-) and the capacitance value C_1 (C_2 being fixed at 5 F m^{-2}).[25] Furthermore, the slip-plane distance, s, was fitted to obtain a good fit to the zeta potential data. Here, we followed previously published procedures.[27] The fitting procedure was performed using a modified version of FITEQL coupled to UCODE.[28,29]

RESULTS AND DISCUSSION

Se(IV) Surface Species on γ-Al_2O_3. To identify oxyanion sorption onto mineral surfaces by vibrational spectroscopy, the knowledge of the spectral fingerprints of the predominant aqueous species is required. With respect to the experimental setup, contributions from aqueous species to the spectra of the sorbed species cannot be ruled out. Thus, the respective spectra obtained for aqueous Se(IV) solutions at selected pD values are provided in Figure 1A serving as references for the spectra obtained

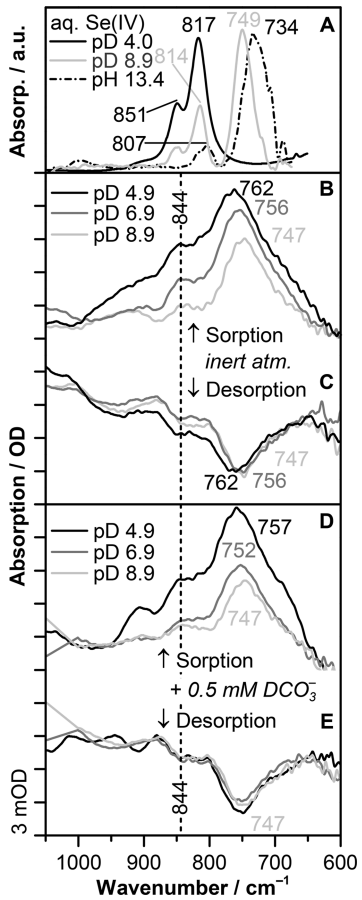

Figure 1. (A) IR spectra of aqueous Se(IV) recorded at pD 4.0 (0.1 mol L^{-1} Se, 0.1 mol L^{-1} NaCl), pD 8.9 (5×10^{-3} mol L^{-1} Se, 0.1 mol L^{-1} NaCl), and pH 13.4 (8.8×10^{-2} mol L^{-1} Se). (B, D) In situ IR spectra of the Se(IV) surface species observed after 60 min of sorption on γ-Al_2O_3 and (C, E) after subsequent flushing with background electrolyte for 60 min (B, C) under inert gas conditions (N_2) and (D, E) in the presence of carbonate (5×10^{-4} mol L^{-1} DCO_3^-) at pD 4.9, 6.9, and 8.9 ($[Se(IV)]_{init.} = 5 \times 10^{-4}$ mol L^{-1}, I = 0.1 M NaCl).

during the sorption and desorption processes (Figures 1B–E). The Se(IV) aqueous speciation (SI Figure S4) as well as a brief assignment of the observed bands to vibrational modes of the Se(IV) species is given in the SI.

The transient spectra recorded for the sorbed species showed increasing amplitudes in the spectral region of the ν(SeO) stretching modes reflecting the accumulation of surface species at the alumina surface (SI Figure S5). In all experiments of this work, the amplitudes generally reached maximum values about 40 min after sorption was initiated indicating that a steady state was obtained. In addition, prolonged sorption up to 120 min revealed no spectral changes ruling out the formation of surface precipitates. Representative spectra recorded after 60 min of sorption are shown in Figure 1B.

The spectra following Se(IV) sorption (Figure 1B) were significantly different from the spectra of the aqueous species (Figure 1A) evidencing the formation of surface species at the alumina surface. Under mildly acidic conditions (pD 4.9), a predominant broad feature was observed showing two maxima at 844 and 762 cm^{-1} representing the $\nu_{1,s}$ and $\nu_{3,as}$(Se–O) modes

DOI: 10.1021/acs.est.7b04546
Environ. Sci. Technol. 2018, 52, 581–588

(see SI).[30] Under more alkaline conditions, the intensity of the bands decreased with increasing pH reflecting a decreased affinity of the Se(IV) anions for the alumina surface most likely due to less favorable electrostatics.

The $\nu_{3,as}$(Se−O) mode was bathochromically shifted to 756 and 747 cm^{-1} with increasing pD (Figure 1B). Such a shift potentially might indicate the formation of another species due to the increased pD. However, the band showed no broadening with increasing pD suggesting that the frequency of the respective vibrational mode is just lowered and no additional mode contributed to this spectral feature. This interpretation was corroborated by spectral decomposition and fitting of the spectra. The results obtained demonstrated that the spectra could be satisfactorily reproduced with only two bands representing two different vibrational modes, one constantly located around 840 cm^{-1} and another slightly shifting from ∼760 to ∼745 cm^{-1} with increasing pD (SI Figure S6). The occurrence of additional species is expected to require further components to obtain adequate fitting results. Thus, the pD depending shifting of the $\nu_{3,as}$(Se−O) mode likely reflects modifications of the alumina surface charge due to the prevailing pD value. Together with the results of the previous EXAFS study of Elzinga et al.[10] which did not reveal the presence of another species related to a second Se−Al distance, the formation of a single predominant Se(IV) species at the alumina surface, independently of the pH, can be assumed with confidence.

Subsequent to sorption, desorption was induced by flushing the alumina film with a 0.1 mol L^{-1} NaCl blank electrolyte solution for 1 h. The respective spectra are shown as negative bands representing species which were released from the mineral phase during the desorption step (Figure 1C). The high congruence of the spectral shapes observed during the sorption and desorption steps strongly suggests that the same Se(IV) species were involved in adsorption and desorption processes. The amplitudes of these spectra were found to be nearly independent of pD indicating an increasing relative reversibility with increasing pD. However, at pD 4.9 the amplitude of the desorption spectra did not exceed ∼55% of the sorption spectra. This rather low reversibility of the sorption reaction indicates predominant formation of inner-sphere complexes under those conditions. Prevalence of outer-sphere complexation was found to result in high reversibility, which is in good agreement with the amplitudes of sorption and desorption spectra in recent in situ ATR FT-IR spectroscopic experiments.[16,31]

To verify the inner-sphere Se(IV)-alumina species suggested in our experiments, we have performed in situ experiments at different ionic strengths (SI Figure S7). Increasing the ionic strength by a factor up to 50 (from 0.01 to 0.5 mol L^{-1}) revealed no significant impact on the resulting spectra irrespective of the pH conditions. This insensitivity of the spectra with ionic strength can be interpreted in terms of predominant formation of inner-sphere complexes, which is in agreement with the observed decrease to more acidic pH value of the isoelectric point of alumina upon Se(IV) sorption.[10,14] While these macroscopic observations are suggestive, the formation of inner-sphere complexes upon Se(IV) sorption onto γ-Al_2O_3 was definitely shown from EXAFS measurements.[10]

The derivation of structural molecular information, such as molecule symmetry and binding mode of surface complexes, from vibrational spectra is potentially accessible due to the correlation between the molecule symmetry and occurring vibrational modes. However, an unequivocal interpretation of the spectral features observed for the Se(IV) surface species is rather difficult due to low molecule symmetry. Such low molecule symmetries generally reveal numerous vibrational modes characterized by weak intensities, broad line widths and poor energetic separation. From vibrational data of SeO_3^{2-} metal complexes it is known that the selenite anion in the complex shows C_s symmetry. This symmetry group is expected for both a monodentate and a bidentate coordination of the selenite anion.[32] Thus, the type of coordination cannot be intrinsically distinguished based on the number of vibrational modes to be observed in the spectra. Moreover, an assignment of mono- and bidentate coordinated SeO_3^{2-} ions by the fingerprint of vibrational modes in IR spectra has not been accurately described up to now. Only the frequency ranges from 805 to 832 cm^{-1} and from 755 to 770 cm^{-1} were identified to show vibrational modes of SeO_3^{2-} ions in metal complexes,[32] which is in agreement with the spectra of the surface complexes of this work (Figure 1B−E). However, previous EXAFS studies reported the formation of bidentate bridging complexes with AlO_6 surface groups onto γ-alumina at circumneutral pH.[10] Thus, the formation of Se(IV) bidentate inner-sphere surface complexes at the alumina surface was assumed.

To gain insight into the sorption processes of Se(IV) under ambient conditions, simultaneous sorption of Se(IV) and DIC was studied. As the IR measurements of the Se(IV) sorption processes had to be performed in D_2O, the atmospherically equimolar amount of DIC was added to the Se(IV) solution as solid $NaDCO_3$, which avoided H_2O contamination. The respective Se(IV) spectra obtained after a prolonged equilibration of the alumina phase under inert gas conditions and subsequent 60 min of incubation are shown in Figure 1D. The experiments were performed at three different pD values. The spectra of the subsequent flushing steps are shown in Figure 1E.

The overall shapes of the spectra are in very good agreement with those obtained in the absence of DIC indicating that the same Se surface species are formed, regardless on DIC presence, which is also supported by the same observed bathochromic shift of the band's maximum with increasing pD. However, the amplitudes of the spectra obtained at increased pD values were reduced in the presence of DIC (Figure 1D). From these findings, it is assumed that prevailing carbonate species hampered the accessibility of Se(IV) to the alumina surface, as the number of available surface sites decreases.

In contrast, the coordination of carbonate on the alumina surface was almost completely suppressed in the presence of 5×10^{-4} mol L^{-1} Se(IV). It was explicitly shown that carbonate ions showed an affinity to the alumina surface in the absence of Se(IV) (SI Figure S8). The high degree of reversibility found for these sorption processes and the spectral characteristics of the carbonate modes suggested the formation of monodentate outer-sphere species at the alumina surface (SI Figure S8). During simultaneous sorption of Se(IV) and DIC, hardly any bands representing DIC were observed reflecting a negligible uptake in the presence of Se(IV) on alumina which corroborates the higher affinity of Se(IV) for the alumina surface (SI Figure S8).

This higher affinity is expected to cause removal of carbonate ions from the surface by Se(IV), provided that both species bind to the same sites. In fact, this assumption was confirmed by an additional experiment where Se(IV) was exposed to the alumina phase which had been allowed to equilibrate with DIC beforehand. The spectral modifications related to Se(IV) sorption processes performed at circumneutral pH are shown in

DOI: 10.1021/acs.est.7b04546
Environ. Sci. Technol. 2018, 52, 581−588

Figure 2A and B for the frequency ranges of the carbonate and Se(IV) modes, respectively.

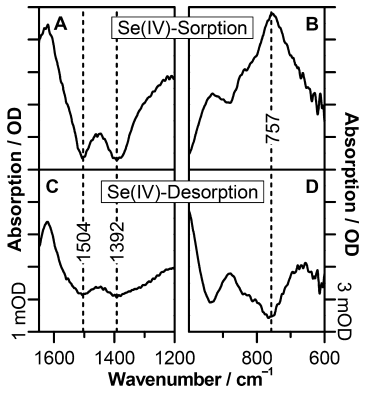

Figure 2. (A, B) In situ IR spectra of Se(IV) sorption process on γ-Al_2O_3 which was preconditioned with atmospherically derived carbonate and (C, D) after subsequent flushing with background electrolyte for 60 min at pD 6.9. (A, C) The spectral regions of the carbonate and (B, D) Se(IV) are shown. Experimental conditions were as given in Figure 1.

The spectra clearly demonstrate that during the sorption processes of Se(IV), characterized by the band at 757 cm^{-1} (Figure 2B), carbonate was released from the alumina surface as reflected by negative bands observed at 1504 and 1392 cm^{-1} (Figure 2A). Thus, it is obvious that Se(IV) replaced carbonate ions on the alumina surface again confirming the higher affinity of Se(IV). Subsequent flushing with pure background electrolyte demonstrated a fractional release of Se(IV) (Figure 2D), which is in accordance with previous results (Figures 1C and E), and with a very small residual amount of remaining carbonate (Figure 2C). The high congruence of vibrational modes of Se(IV) throughout the spectra of the sorption and desorption processes strongly suggests the formation of a single predominant inner-sphere surface species on alumina irrespective of the conditions (i.e., inert or DIC containing solutions). Although the derivation of detailed molecule symmetries from the spectral fingerprinting is not feasible given the current state of knowledge, a bidentate coordination of the anion to the surface is assumed as suggested from earlier investigations.[10] These qualitative findings constitute a prerequisite for the comprehensive description of the sorption system Se(IV)/γ-Al_2O_3 studied by batch sorption experiments and thermodynamic modeling.

Surface Acid–base Behavior, Zeta Potentials, and Modeling. To model the Se(IV) adsorption data successfully, the determination of the acid–base parameters of the solid phase is required. The experimental titration results (surface charge density vs pH) at different ionic strengths are shown in Figure 3A, while zeta potential measurements as a function of pH are given in Figure 3B. Solid lines show the modeling results in each figure. The reactions used and the corresponding obtained parameters are summarized in Table 1. The capacitance C_1 and the parameter x were 1.39 F m^{-2} and 0.44, respectively. The fitted parameter x is related to the slip plane distance s and the ionic strength dependent Debye length κ by $x = s \times \kappa$.[33]

As it can be seen in Figure 3A, a satisfactory description of the titration data is obtained with a one site and a three plane model. The pH_{IEP} of γ-Al_2O_3, located at pH 9.0, was insensitive to the background electrolyte concentration (Figure 3B), suggesting the identical or absence of stronger adsorption of Na or Cl to γ-Al_2O_3. The potentiometric data derived in the present

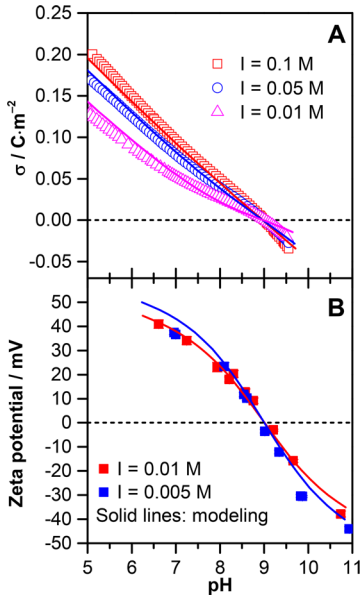

Figure 3. (A) Surface charge of the neat surface of γ-Al_2O_3 (m/v = 20 g L^{-1}, I = 0.01, 0.05, and 0.1 mol L^{-1} NaCl) (□, ○, Δ experiment; fit). (B) Zeta potential of the neat surface of γ-Al_2O_3 (m/v = 0.25 g L^{-1}, I = 0.005 and 0.01 mol L^{-1} NaCl) (■ experiment; fit).

work were compared with former literature studies (SI Figures S9 and S10). A comparison of the results with literature shows that the pH_{IEP} of the present study agrees very well with literature data. Indeed, compilations of Kosmulski[7,34] show that the major part of the PZCs/IEPs of alumina are in the range between pH 8 and 10. Some gamma-alumina data show the very same value that we have obtained. The zeta potential curves and the pH_{IEP} were rather well described (Figure 3B). Charge penetration of the electrolyte ions in the plane 0 or 1 as proposed earlier did not significantly improve the quality of the fit.[25] Consequently, this model was accepted and used further for the modeling of the Se(IV) adsorption data.

Batch Sorption Studies, Zeta Potentials, and Modeling. The amount of Se(IV) sorbed onto γ-Al_2O_3 decreased with increasing pH (Figure 4A). This sorption trend with pH is observed typically in anion retention on metal oxides, since when increasing pH, the surface of the mineral becomes more negative and solid-anion interaction is hindered due to electrostatic repulsion.[35] Raising the ionic strength from 0.01 mol L^{-1} to 0.1 mol L^{-1} NaCl did not significantly impact the Se(IV) sorption, which was already observed[10] and supports the formation of inner-sphere complexes.[10,24]

No significant shift of the pH_{IEP} toward more acidic pH values was observed after addition of 10^{-5} mol L^{-1} of Se(IV) (Figure 4B). However, a clear shift of the pH_{IEP} from 9.0 to 8.1–8.2 occurred with 10^{-4} mol L^{-1} of Se(IV), at the two ionic strengths used (Figure 4B). The decrease of alumina pH_{IEP} was also observed at similar Se(IV) concentrations[10,14] and agrees with the formation of Se(IV) inner-sphere surface complexes.[10,24,36]

The parameters from the acid–base model were kept constant for the Se(IV)-adsorption model. The model involves the assumptions that (i) the Se adsorption does not affect the slip-plane distance and (ii) both inner and outer layer capacitance are not changed by Se adsorption.

For several reasons, such as, for example, the lack of knowledge on the exact position of the slipping plane, we did not intend to perfectly reproduce the zeta potential values upon Se(IV) adsorption.[36] We rather focused on reproducing the

DOI: 10.1021/acs.est.7b04546
Environ. Sci. Technol. 2018, 52, 581–588

Table 1. Parameters for the Surface Species in the Best-Fit Model (Surface Acid–base Properties and Se(IV) Adsorption)

surface species	Δz_0	Δz_1	Δz_2	reaction	log K
surface acid–base properties					
$\equiv AlOH^{-0.5}$	0	0	0		0
$\equiv AlOH_2^{+0.5}$	1	0	0	$\equiv AlOH^{-0.5} + H^+ \rightleftharpoons \equiv AlOH_2^{+0.5}$	9.0
$\equiv AlOH^{-0.5}\cdots Na^+$	0	0	1	$\equiv AlOH^{-0.5} + Na^+ \rightleftharpoons \equiv AlOH^{-0.5}\cdots Na^+$	−0.096
$\equiv AlOH^{+0.5}\cdots Cl^-$	0	0	−1	$\equiv AlOH_2^{+0.5} + Cl^- \rightleftharpoons \equiv AlOH_2^{+0.5}\cdots Cl^-$	−0.176
Se(IV) adsorption					
$[\{(\equiv AlO)(\equiv AlOH)\}SeO]^0$	2.21	−1.21	0	$2(\equiv AlOH^{-0.5}) + 3H^+ + SeO_3^{2-} \rightleftharpoons [\{(\equiv AlO)(\equiv AlOH)\}SeO]^0 + 2H_2O$	30.0

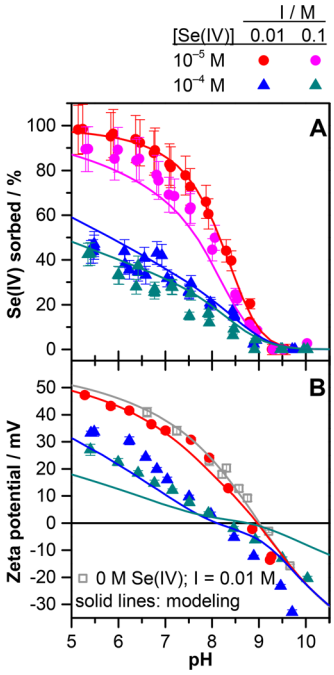

Figure 4. (A) Se(IV) sorption edges onto γ-Al_2O_3 ($[Se^{IV}]_{initial}$ = 1 × 10^{-5} and 1 × 10^{-4} mol L^{-1}, I = 0.1 and 0.01 mol L^{-1} NaCl; ●, ▲ experiment; fit). (B) Zeta potential of the surface of γ-Al_2O_3 ($[Se^{IV}]_{initial}$ = 0, 1 × 10^{-5} and 1 × 10^{-4} mol L^{-1}, 0.1 and 0.01 mol L^{-1} NaCl). (●, ▲, □ experiment; fit). Mass/volume ratio: m/v = 0.25 g L^{-1}, 3 days of shaking under N_2 was chosen for all experiments.

pH_{IEP} and its shift due to interaction with Se(IV). The aqueous Se(IV) protonation constants were taken from the NEA-TDB book for selenium.[3]

$$SeO_3^{2-} + H^+ \rightleftharpoons HSeO_3^-,\ \log K = 8.36$$

$$SeO_3^{2-} + 2H^+ \rightleftharpoons H_2SeO_3,\ \log K = 11.00$$

To design a Se-adsorption model, we started from a previously published Se(IV)-goethite model, that is, a three-plane electrostatic model.[36,37] The spectroscopic data suggested one bidentate surface complex and we therefore used only one surface species (cf. Table 1), namely $[\{(\equiv AlO)(\equiv AlOH)\}SeO]^0$. The interaction between the Se(IV) and the surface of γ-Al_2O_3 was assumed to involve the singly coordinated hydroxyl groups only. The location of the Se(IV) charge at the interface was described via the charge distribution factor. This resulted for the single surface complex in two adjustable parameters (the log K and its respective CD-factor).

Since no shift of the isoelectric point upon Se(IV) adsorption was experimentally observed upon increasing the NaCl concentration, it was not necessary to include sodium binding to the adsorbed Se(IV) in the bidentate surface complex involved in the model, as proposed for the phosphate/goethite binary system.[38] The model is summarized in the following reaction equation and the model fit to the batch data is shown in Figure 4.

$$2(\equiv AlOH^{-0.5}) + 3H^+ + SeO_3^{2-} \rightleftharpoons [\{(\equiv AlO)(\equiv AlOH)\}SeO]^0 + 2H_2O,\ \log K = 30.0.$$

The model describes the adsorption data satisfactorily, except for a slight underestimation at 10^{-5} mol L^{-1} Se(IV) and I = 0.1 mol L^{-1}. The predominance of a bidentate surface species is in full agreement with previous studies.[36,37]

Figure 4B shows the model description of the zeta potentials of the sorbent in absence and presence of Se(IV). The model accurately describes the shift of the pH_{IEP}, although not perfectly. It slightly underestimates the shift of the pH_{IEP} of γ-Al_2O_3 at 10^{-4} mol L^{-1} Se(IV) and I = 0.1 mol L^{-1}. However, we think that the model is adequate since it captures the experimental observations and does not disagree with the spectroscopic data.

Other model options tested (deprotonated bidentate species $[(\equiv AlO)_2SeO]^-$ with or without coadsorption of sodium) did not improve the fit. The model used to calculate the lines in Figure 4 and considering the $[\{(\equiv AlO)(\equiv AlOH)\}SeO]^0$ species was the one that yielded the best fit among all the variations tested. The CD values are related to the position of the proton in the bidentate surface complex. The modeling outcome showed that the obtained CD factor makes sense with the proton close to the surface and not on the "free" oxygen that is oriented toward the solution (an oxygen which would have little proton affinity). The surface complex might be interpreted as involving a hydrogen bond with a neighboring oxygen, as for example discussed by Loring et al.[39] This interpretation necessarily remains tentative and is based on best fit. On the sorbent a sound structural assignment becomes difficult because the surface structure is not known. As such the obtained parameters and stoichiometries can also be understood as the best-fit results, which do not contradict the spectroscopic data. When the parameter x was also fitted, a much better description of the experimental zeta potential values was obtained at 10^{-4} mol L^{-1} Se(IV), while the zeta potentials at 10^{-5} mol L^{-1} Se(IV) were slightly overestimated. Using this value for x to simulate the acid–base surface properties of alumina did not have major effects (SI Figures S11 and S12), besides a slight overestimation of the zeta potentials of the neat alumina surface at acidic pH.

DOI: 10.1021/acs.est.7b04546
Environ. Sci. Technol. 2018, 52, 581–588

ENVIRONMENTAL IMPLICATIONS

Although the most important exposure route to humans is food, exposure to low-level selenium containing drinking water (<10 $\mu g\ L^{-1}$) has been reported to induce severe health effects.[2] A detailed knowledge of the mobility and bioavailability of selenium is therefore of great importance for a safe disposal of radioactive waste as well as for the optimization of decontamination processes of polluted sites.

A reliable description of the interaction at the solid/liquid interface can only be achieved based on a multicomponent approach including adsorption data, spectroscopic characterization and thermodynamic modeling, as shown in this study. This work revealed the interaction of Se(IV) with γ-Al_2O_3 nanoparticles, not occurring naturally, but serving as a model for clay minerals. Since the interaction of Se(IV) with γ-alumina nanoparticles was evidenced to proceed via the formation of strong covalent bonds, stable surface complexes are to be expected at the solid surface. Alumina nanoparticles in ground- or waste-waters might therefore transport and enhance selenium migration in the environment. In natural systems, competitive effects with ubiquitous species such as carbonate ions have to be considered as well. Indeed, they can hinder the adsorption by reducing the availability of surface sites. At higher pH levels, dissolved carbonate ions impede the adsorption of Se(IV) at alumina phases, which can in turn increase the mobility of Se in the environment. These results can be implemented in reactive transport models to improve the monitoring of the environmental fate of selenium. An accurate description of the carbonate interaction with alumina surfaces including batch studies and thermodynamic modeling is also of high environmental relevance and will be the scope of future studies.

ASSOCIATED CONTENT

Supporting Information

The Supporting Information is available free of charge on the ACS Publications website at DOI: 10.1021/acs.est.7b04546.

It contains detailed descriptions concerning the characterization of γ-Al_2O_3, the preparation of the solutions, the aqueous speciation of Se(IV) and carbonate ions, the performance of the in situ ATR FT-IR measurements (impact of pD, ionic strength and dissolved inorganic carbon), spectral fitting results of the sorption spectra obtained, a comparison with former potentiometric titration as well as details about surface complexation modeling (PDF)

AUTHOR INFORMATION

Corresponding Authors

*(N. J.) Phone: +49 351 260 2148, e-mail: N.Jordan@hzdr.de.
*(H. F.) Phone: +49 351 260 3664, e-mail: foersten@hzdr.de.

ORCID

Harald Foerstendorf: 0000-0002-8334-9317
Katja Schmeide: 0000-0002-6859-8366
Norbert Jordan: 0000-0002-4625-1580

Author Contributions

The manuscript was written through contributions of all authors. All authors have given approval to the final version of the manuscript. NJ and HF are the lead authors from Helmholtz-Zentrum Dresden - Rossendorf.

Notes

The authors declare no competing financial interest.

ACKNOWLEDGMENTS

This work has been partially supported by MIRAME (CTM-2014-60482-P) Spanish Ministry of Economy and Competitiveness project. N.M. acknowledges FPI BES-2012-056603 and EEBB-I-15-09446 grants, both from MINECO (Spain). Dr. Luis Gutiérrez Nebot from CIEMAT and Dr. Atsushi Ikeda-Ohno are acknowledged for XRD measurements. Birke Pfützner, Heidrun Neubert, Christa Müller and Salim Shams Aldin Azzam are acknowledged for support during batch, zeta potential and ICP-MS measurements.

REFERENCES

(1) Fernández-Martínez, A.; Charlet, L. Selenium environmental cycling and bioavailability: a structural chemist point of view. *Rev. Environ. Sci. Bio/Technol.* **2009**, *8* (1), 81−110.

(2) *Selenium in Drinking-Water. Background Document for Development of WHO Guidelines for Drinking-Water Quality*; World Health Organization: Geneva, 2011.

(3) Olin, A.; Noläng, B.; Osadchii, E. G.; Öhman, L.-O.; Rosén, E. *Chemical Thermodynamics of Selenium*; Elsevier: Amsterdam, 2005.

(4) Trueba, M.; Trasatti, S. P. γ−Alumina as a support for catalysts: A review of fundamental aspects. *Eur. J. Inorg. Chem.* **2005**, *17*, 3393−3403.

(5) Levin, I.; Brandon, D. Metastable alumina polymorphs: Crystal structures and transition sequences. *J. Am. Ceram. Soc.* **1998**, *81* (8), 1995−2012.

(6) Sposito, G. *Chemical equilibrium and Kinetics in soils*, First ed.. Oxford University Press, New York, 1994.

(7) Kosmulski, M. The pH-dependent surface charging and points of zero charge V. Update. *J. Colloid Interface Sci.* **2011**, *353* (1), 1−15.

(8) Mayordomo, N.; Alonso, U.; Missana, T. Analysis of the improvement of selenite retention in smectite by adding alumina nanoparticles. *Sci. Total Environ.* **2016**, *572*, 1025−1032.

(9) Lagaly, G.; Dékány, I., Colloid Clay Science. In *Handbook of Clay Science*, 2nd ed.; Elsevier: Amsterdam, The Nederlands, 2013.

(10) Elzinga, E. J.; Tang, Y. Z.; McDonald, J.; DeSisto, S.; Reeder, R. J. Macroscopic and spectroscopic characterization of selenate, selenite, and chromate adsorption at the solid-water interface of γ-Al_2O_3. *J. Colloid Interface Sci.* **2009**, *340* (2), 153−159.

(11) Balistrieri, L. S.; Chao, T. T. Selenium adsorption by goethite. *Soil Science Society of America Journal* **1987**, *51* (5), 1145−1151.

(12) Fujikawa, Y.; Fukui, M. Radionuclide sorption to rocks and minerals: Effects of pH and inorganic anions 0.1. Sorption of cesium, cobalt, strontium and manganese. *Radiochim. Acta* **1997**, *76* (3), 153−162.

(13) Kim, S. S.; Min, J. H.; Lee, J. K.; Baik, M. H.; Choi, J. W.; Shin, H. S. Effects of pH and anions on the sorption of selenium ions onto magnetite. *J. Environ. Radioact.* **2012**, *104*, 1−6.

(14) Missana, T.; Benedicto, A.; Mayordomo, N.; Alonso, U. Analysis of anion adsorption effects on alumina nanoparticles stability. *Appl. Geochem.* **2014**, *49*, 68−76.

(15) Foerstendorf, H.; Jordan, N.; Heim, K. Probing the surface speciation of uranium (VI) on iron (hydr)oxides by *in situ* ATR FT-IR spectroscopy. *J. Colloid Interface Sci.* **2014**, *416*, 133−138.

(16) Jordan, N.; Ritter, A.; Foerstendorf, H.; Scheinost, A. C.; Weiss, S.; Heim, K.; Grenzer, J.; Mücklich, A.; Reuther, H. Adsorption mechanism of selenium(VI) onto maghemite. *Geochim. Cosmochim. Acta* **2013**, *103*, 63−75.

(17) Lefèvre, G. *In situ* Fourier-transform infrared spectroscopy studies of inorganic ions adsorption on metal oxides and hydroxides. *Adv. Colloid Interface Sci.* **2004**, *107* (2−3), 109−123.

(18) Carrier, X.; Marceau, E.; Lambert, J. F.; Che, M. Transformations of gamma-alumina in aqueous suspensions 1. Alumina chemical weathering studied as a function of pH. *J. Colloid Interface Sci.* **2007**, *308* (2), 429−437.

(19) Dyer, C.; Hendra, P. J.; Forsling, W.; Ranheimer, M. Surface hydration of aqueous γ-Al_2O_3 studied by Fourier transform Raman and

DOI: 10.1021/acs.est.7b04546
Environ. Sci. Technol. 2018, 52, 581−588

infrared spectroscopy—I. Initial results. *Spectrochimica Acta Part a-Molecular and Biomolecular Spectroscopy* **1993**, *49* (5−6), 691−705.
(20) Laiti, E.; Persson, P.; Ohman, L. O. Balance between surface complexation and surface phase transformation at the alumina/water interface. *Langmuir* **1998**, *14* (4), 825−831.
(21) Lefèvre, G.; Duc, M.; Lepeut, P.; Caplain, R.; Fedoroff, M. Hydration of γ-alumina in water and its effects on surface reactivity. *Langmuir* **2002**, *18* (20), 7530−7537.
(22) Wijnja, H.; Schulthess, C. P. ATR-FTIR and DRIFT spectroscopy of carbonate species at the aged γ-Al_2O_3/water interface. *Spectrochim. Acta, Part A* **1999**, *55* (4), 861−872.
(23) Glasoe, P. K.; Long, F. A. Use of glass electrodes to measure acidities in deuterium oxide. *J. Phys. Chem.* **1960**, *64* (1), 188−190.
(24) Jordan, N.; Ritter, A.; Scheinost, S. Selenium(IV) Uptake by Maghemite (γ-Fe_2O_3). *Environ. Sci. Technol.* **2014**, *48* (3), 1665−1674.
(25) Hiemstra, T.; Yong, H.; Van Riemsdijk, W. H. Interfacial charging phenomena of aluminum (hydr)oxides. *Langmuir* **1999**, *15* (18), 5942−5955.
(26) Hiemstra, T.; Van Riemsdijk, W. H.; Bolt, G. H. Multisite proton adsorption modeling at the solid/solution interface of (hydr)oxides: A new approach: I. Model description and evaluation of intrinsic reaction constants. *J. Colloid Interface Sci.* **1989**, *133* (1), 91−104.
(27) Bouby, M.; Lützenkirchen, J.; Dardenne, K.; Preocanin, T.; Denecke, M. A.; Klenze, R.; Geckeis, H. Sorption of Eu(III) onto titanium dioxide: Measurements and modeling. *J. Colloid Interface Sci.* **2010**, *350* (2), 551−561.
(28) Westall, J. C. *FITEQL: A Computer Program for Determination of Chemical Equilibrium Constants from Experimental Data*; Department of Chemistry, Oregon State University: Corvallis, OR, 1982.
(29) Poeter, E. P.; Hill, M. C. *Documentation of UCODE: A Computer Code for Universal Inverse Modeling*, 1998.
(30) Kretzschmar, J.; Jordan, N.; Brendler, E.; Tsushima, S.; Franzen, C.; Foerstendorf, H.; Stockmann, M.; Heim, K.; Brendler, V. Spectroscopic evidence for selenium(IV) dimerization in aqueous solution. *Dalton Transactions* **2015**, *44* (22), 10508−10515.
(31) Jordan, N.; Foerstendorf, H.; Weiss, S.; Heim, K.; Schild, D.; Brendler, V. Sorption of selenium(VI) onto anatase: Macroscopic and microscopic characterization. *Geochim. Cosmochim. Acta* **2011**, *75* (6), 1519−1530.
(32) Fowless, A. D.; Stranks, D. R. Selenitometal Complexes. 1. Synthesis and Characterization of Selenito Complexes of Cobalt (III) and Their Equilibrium Properties in Solution. *Inorg. Chem.* **1977**, *16* (6), 1271−1276.
(33) Lützenkirchen, J.; Preocanin, T.; Kallay, N. A macroscopic water structure based model for describing charging phenomena at inert hydrophobic surfaces in aqueous electrolyte solutions. *Phys. Chem. Chem. Phys.* **2008**, *10* (32), 4946−4955.
(34) Kosmulski, M. *Surface Charging and Points of Zero Charge*; CRC Press, 2009; Vol. *145*.
(35) Szczepaniak, W.; Koscielna, H. Specific adsorption of halogen anions on hydrous γ-Al_2O_3. *Anal. Chim. Acta* **2002**, *470* (2), 263−276.
(36) Nie, Z.; Finck, N.; Heberling, F.; Pruessmann, T.; Liu, C. L.; Lützenkirchen, J. Adsorption of Selenium and Strontium on Goethite: EXAFS Study and Surface Complexation Modeling of the Ternary Systems. *Environ. Sci. Technol.* **2017**, *51* (7), 3751−3758.
(37) Hiemstra, T.; Rietra, R.; Van Riemsdijk, W. H. Surface complexation of selenite on goethite: MO/DFT geometry and charge distribution. *Croatica Chemica Acta* **2007**, *80* (3−4), 313−324.
(38) Rahnemaie, R.; Hiemstra, T.; van Riemsdijk, W. H. Geometry, charge distribution, and surface speciation of phosphate on goethite. *Langmuir* **2007**, *23* (7), 3680−3689.
(39) Loring, J. S.; Sandström, M. H.; Norén, K.; Persson, P. Rethinking Arsenate Coordination at the Surface of Goethite. *Chem. - Eur. J.* **2009**, *15* (20), 5063−5072.

DOI: 10.1021/acs.est.7b04546
Environ. Sci. Technol. 2018, 52, 581−588